A Comparison of Calculation by Real-Time and by Linear-Response Time-Dependent Density Functional Theory in the Regime of Linear Optical Response

THESIS

Presented in Partial Fulfillment of the Requirements for
the Degree Master of Science in the Graduate
School of The Ohio State University

By

Ying Zhu, B.S.

Graduate Program In Chemical Physics
The Ohio State University

2016

Thesis Committee:

John M. Herbert, Adviser

Louis F. DiMauro

Christopher J. Jaroniec

Abstract

We present a method to calculate the excited electronic structure of chemical systems via a real-time approach by using time-dependent density functional theory (TDDFT), i.e. real-time TDDFT. The conventional approach of TDDFT is solving the linear response in frequency domain, which we denote here as linear-response TDDFT (LR-TDDFT). Real-time TDDFT (RT-TDDFT) is calculated by integrating the propagation over the time. Detailed deduction and algorithms of RT-TDDFT are discussed. The computation algorithms of the pilot codes for the RT-TDDFT implementation [1] in the Q-Chem quantum chemistry software package is thoroughly checked. The codes of RT-TDDFT are merged into the main develop version of Q-Chem. The computation results are compared between LR-TDDFT and RT-TDDFT. The results show a good match between LR-TDDFT and RT-TDDFT calculation. This proves the validity of RT-TDDFT calculation implementation and prepare us for the future study on the excited states electronic structure and dynamics via the real-time approach.

Vita

2013	B.S. Applied Physics, Univerisity of Science and Technology of China
2013-2015	Graduate Teaching Associate, The Ohio State University
2016-present	Graduate Research Associate, The Ohio State University

Fields of Study

Major Field: Chemical Physics, Theoretical Chemistry

Table of Contents

List of Figures

CHAPTER 1

Introduction

1.1 Overview

The study on electronic structure and excited states dynamics of molecular systems is crucial to understand mechanisms of photochemistry, electrochemistry, chemical interaction,etc. A detailed understanding of such not only satisfies human curiosity in the molecular level, but also shed light on and expedite applicable ways such as finding materials with electrical/photo-efficiency and preventing photo lesion formations for biological systems.

In the study of the electronic structure of many-electron systems, there are two major approaches. The first one is solving the many-body Shrödinger equation by finding solutions to the wave functions, which is illustrated as Hartree-Fock (HF) theory. The other one is finding solutions to the density distribution instead, therefore obtains values of other observables. The latter is stated as density functional theory (DFT)[3][4] for the ground state calculation, and generalized into the excited state calculation in time-dependent density functional theory (TDDFT)[5][6][7]. Because of its computational efficiency and accuracy of the solution, DFT has gained increasing popularity in chemical physics society since 1980s, and now is being widely used[8].

On the top of TDDFT, there are two computational approaches. The first one, which is already most widely used and often referred to directly as TDDFT in literatures, solves many-body quantum problems in the frequency domain via Fourier transformation of the time-dependent linear response function, and obtains excitation energies and corresponding oscillation strengths from poles and residues in the complex response function. In order to distinguish this approach from the second one, it is referred to as linear-response TDDFT (LR-TDDFT) [9][10].

The second approach solves the problem, which mathematically is a partial differential equation , by integrating over the time and space. Since it is calculated step-by-step in the time domain, it is referred as real-time TDDFT (RT-TDDFT)[11][12][13][14].

Both approaches have advantages and disadvantages. For the LR-TDDFT, it is usually computational efficient. By implementing Davidson iteration method, the few low-lying excited states can be easily obtained with a low computational cost. However, the storage demand is relatively high, and the calculation is limited to the weak perturbation field to meet the requirement of the linear-response approximation. For the RT-TDDFT, on the contrary, is computational costly, for the reason that integration over time requires large amount of calculation. However, the storage requirement is much lower, and its validity does not limit to the weak field. What's more, dynamics of the system can be obtained directly.

Because of the computational efficiency, LR-TDDFT is the mostly implemented

scheme in quantum chemistry calculation software packages. On the contrary, RT-TDDFT is only implemented in a few packages. However, considering the complementary advantages of RT-TDDFT compared with LR-TDDFT, it is worthwhile developing RT-TDDFT to study cases like large molecules systems which are previously prohibited by the computation storage limitation, chemical systems in a strong external fields, and the dynamics of the systems in the ultra-fast regime.

In the remaining of this chapter , we briefly introduce density functional theory (DFT), time-dependent density functional theory (TDDFT), linear-response time-dependent density functional theory (LR-TDDFT), and the trade-off between memory (storage) and CPU time. In chapter two, details of RT-TDDFT implementation are provided, such as the deductions of equation of motion, the use of transformation of basis, the calculation of the time-dependent Fock matrix, and the algorithms of the propagator. In chapter three, the results calculated by RT-TDDFT and LR-TDDFT are compared in the linear optical response limit. And in chapter four, the conclusion is provided.

1.2 Density Functional Theory (DFT)

The theoretical foundation of DFT is formed by Hohenberg, Kohn and Sham during 1964-1965. For an N-electron system, the electronic Shrödinger equation is

$$H\Psi\left(\mathbf{r}_1, \mathbf{r}_2, \mathbf{r}_3, ..., \mathbf{r}_{N-1}, \mathbf{r}_N\right) = E\Psi\left(\mathbf{r}_1, \mathbf{r}_2, \mathbf{r}_3, ..., \mathbf{r}_{N-1}, \mathbf{r}_N\right), \tag{1.1}$$

with Hamiltonian as

$$H = -\frac{1}{2}\sum_i \nabla_i^2 + \frac{1}{2}\sum_{j\neq i}\sum_i \frac{1}{\|\mathbf{r}_i - \mathbf{r}_j\|} + \sum_i v_{ext}\left(\mathbf{r}_i\right), \tag{1.2}$$

where $\Psi\left(\mathbf{r}_1, \mathbf{r}_2, \mathbf{r}_3, ..., \mathbf{r}_{N-1}, \mathbf{r}_N\right)$ is the electronic wave function representing all N electrons at position $\mathbf{r}_1, \mathbf{r}_2, \mathbf{r}_3, ..., \mathbf{r}_{N-1}, \mathbf{r}_N$ respectively, and the external potential v_{ext} contains the coulomb potential provided by nucleus and the external field.

The unit used here is atomic units (a.u.), i.e. in such units, $\hbar = e = 4\pi\epsilon_0 = m_e = 1$. Some conversions between a.u. and SI unit are listed here.

	atomic unit	SI unit
Time	1 a.u	0.02419 fs
Length	1 a.u	0.5292 Å
Energy	1 a.u	27.2114 eV
Dipole moment	1 a.u	2.542 D

The traditional way in quantum mechanics to solve electronic states for electrons systems is by setting up the corresponding Schrödinger equation, and finding solutions to the wave functions. Then observables, such as density distribution $\rho\left(\mathbf{r}\right)$, can be therefore calculated. For the ground state calculation, the logic goes as that external field v_{ext} determines the ground state wave function Ψ_0 to obtains observables $\mathcal{O}$, such as density distribution ρ, i.e. $\rightarrow v_{ext} \rightarrow \Psi_0 \rightarrow \mathcal{O}$.

Density Functional Theory provides an alternative way. In DFT, the electronic structure is solved by finding the possible electron density distribution $\rho(r)$ for the ground state, without calculate the wave function. The validity of this approach is proved by the first Hohenberg-Kohn theorem (the existence theorem). And the method to obtain such density distribution $\rho(r)$ is stated in the second Hohenberg-Kohn theorem.

In the first Hohenberg-Kohn theorem, the mapping from v_{ext} to the ground state electron density distribution $\rho(r)$ is proved to be a one-to-one mapping. Conversely speaking, the electronic properties of the system are determined by the ground state electron density distribution $\rho(r)$. Consider that observables are determined by wave functions, and the wave functions are determined by v_{ext}. Therefore, by $\rho(r)$, values of observables can be calculated. The logic goes like: $\rho \to v_{ext} \to \Psi_0 \to \mathcal{O}$.

In the second Hohenberg-Kohn theorem (the variation theorem), ground state electron density distribution $\rho(r)$ is proved that can be obtained by the variation that

$$\frac{\delta E\left[\rho\right]}{\delta \rho\left(\mathbf{r}\right)} = 0, \tag{1.3}$$

for the reason that the ground state $\rho(r)$ must correspond to the minimum of energy. Energy represented by $\rho(r)$ is

$$\begin{aligned} E\left[\rho\right] &= \langle \tilde{\Psi}\left[\rho\right] | H | \tilde{\Psi}\left[\rho\right] \rangle \\ &= T\left[\rho\right] + V_{ee}\left[\rho\right] + \int \rho\left(\mathbf{r}\right) v_{ext}\, \mathrm{d}\mathbf{r}. \end{aligned} \tag{1.4}$$

$T\left[\rho\right]$ is the collection of kinetic energy of all electrons. $V_{ee}\left[\rho\right]$ is the collection of electric potential energy between electrons which includes all electron-electron interaction. v_{ext} is the electric field provided by atomic nucleus. To note here, $T\left[\rho\right]$ and $V_{ee}\left[\rho\right]$ are exact and they are functions of density distribution ρ, but the explicit analytic expression is unknown. Thus, by doing the variation as in eq 1.3, ρ for the ground state is obtained.

Based on the above two theorems, Kohn and Sham took a further step to break down the density distribution $\rho(\mathbf{r})$ into fictitious N independent wave functions for

each of the electrons, while assume the existence of the fictitious independent electron system that yields the same density distribution $\rho(\mathbf{r})$ as the actual electron system. Those wave functions are not actual and the electronic correlation (entanglement between electrons) is not considered. The benefits of adapting such fictitious system come as two parts. First, the expression of kinetic term and the coulomb electron-electron interaction for such fictitious system is known. Second,the preceding developed algorithms, which has been used in wave functions quantum chemistry calculation, can be adapted into DFT calculation.

For more details, we assume $\Psi_{non-inter}$ as the total wave function for the fictitious non-interacting independent system, and we refer to that as a reference system. Define the exchange-correlation energy E_{xc} as the difference of the kinetic energy and the electron interactions between those in the actual system and those in the reference system, i.e.

$$\begin{aligned} E_{xc}\left[\rho\left\{\Psi_{non-inter}\right\}\right] \equiv & \left(T\left[\rho\left\{\Psi_{inter}\right\}\right] - T\left[\rho\left\{\Psi_{non-inter}\right\}\right]\right) \\ & + \left(E_{ee}\left[\rho\left\{\Psi_{inter}\right\}\right] - J\left[\rho\left\{\Psi_{non-inter}\right\}\right]\right), \end{aligned} \tag{1.5}$$

where each term is the functional of the density distribution $\rho(\mathbf{r})$. $T\left[\rho\left\{\Psi_{inter}\right\}\right]$ is the exact kinetic energy for the actual system. $T\left[\rho\left\{\Psi_{non-inter}\right\}\right]$ is the kinetic energy for the reference system. $E_{ee}\left[\rho\left\{\Psi_{inter}\right\}\right]$ is the exact electron-electron energy for the actual system. And $J\left[\rho\left\{\Psi_{non-inter}\right\}\right]$ is the Coulomb potential energy for the reference system.

The total wave function $\Psi_{non-inter}$ is represented in the form of Slater determinant

composed of orthonormal wave functions $\{\psi_i\}$ for each of the electron:

$$\Psi_{non-inter} = \frac{1}{\sqrt{N!}} \begin{vmatrix} \psi_1(\mathbf{x}_1) & \psi_2(\mathbf{x}_1) & \psi_3(\mathbf{x}_1) & \dots & \psi_N(\mathbf{x}_1) \\ \psi_1(\mathbf{x}_2) & \psi_2(\mathbf{x}_2) & \psi_3(\mathbf{x}_2) & \dots & \psi_N(\mathbf{x}_2) \\ \vdots & \vdots & \vdots & \ddots & \vdots \\ \psi_1(\mathbf{x}_N) & \psi_2(\mathbf{x}_N) & \psi_3(\mathbf{x}_N) & \dots & \psi_N(\mathbf{x}_N) \end{vmatrix}. \tag{1.6}$$

The wave functions $\{\psi_i\}$ are referred to as orbitals, or as molecular orbitals (MO). $\mathbf{x}_i$ is the vector that contains position $\mathbf{r}$ and spin. The total density is

$$\rho = \sum_i^{N_{MO}} |\psi_i|^2. \tag{1.7}$$

The total energy is

$$\begin{aligned} E[\rho(\mathbf{r})] =& T_{exact}[\rho] + V_{ee}[\rho] + E_{ext}[\rho] \\ =& T_{non-inter}[\rho] + J[\rho] + E_{xc}[\rho] + E_{ext}[\rho], \end{aligned} \tag{1.8}$$

where

$$T_{non-inter}[\rho] = -\frac{1}{2} \sum_i^{N_{MO}} \langle \psi_i | \nabla_i^2 | \psi_i \rangle, \tag{1.9}$$

$$J(\rho) = \frac{1}{2} \sum_i^{N_{MO}} \sum_j^{N_{MO}} \int\int |\psi_i(\mathbf{r}_1)|^2 \frac{1}{\mathbf{r}_{12}} |\psi_j(\mathbf{r}_2)|^2 d\mathbf{r}_1 d\mathbf{r}_2, \tag{1.10}$$

$$E_{ext}[\rho] = \int \rho(\mathbf{r}) V_{ext} d\mathbf{r} = -\sum_i^{N_{MO}} \int \sum_A^M \frac{Z_A}{r_{1A}} |\psi_i(\mathbf{r_1})|^2 d\mathbf{r_1}. \tag{1.11}$$

In the summation of eq 1.11, symbol A refers to a nuclei, and symbol M is total number of nucleus. Thus, we have

$$\begin{aligned} E[\rho(\mathbf{r})] =& -\frac{1}{2} \sum_i^N \langle \psi_i | \nabla_i^2 | \psi_i \rangle + \frac{1}{2} \sum_i^N \sum_j^N \int\int |\psi_i(\mathbf{r}_1)|^2 \frac{1}{\mathbf{r}_{12}} |\psi_j(\mathbf{r}_2)|^2 d\mathbf{r}_1 d\mathbf{r}_2 \\ &+ E_{xc}[\rho\{\Psi_{non-inter}\}] - \sum_i^N \int \sum_A^M \frac{Z_A}{r_{1A}} |\psi_i(\mathbf{r}_1)|^2 d\mathbf{r}_1. \end{aligned} \tag{1.12}$$

By taking the variation according to the second Hohenberg-Kohn theorem, it can be separated into N equations for each of orbitals, which is called as Kohn-Sham (KS) equation:

$$-\frac{1}{2}\nabla^2\psi_i + v_{ks}\psi_i = \varepsilon_i\psi_i, \tag{1.13}$$

$$v_{ks} = v_{ext} + v_{el} + \frac{\delta E_{xc}}{\delta\rho}. \tag{1.14}$$

v_{ks} is Kohn-Sham effective potential, and it has the dependence on overall density distribution $\rho(\mathbf{r})$.

1.3 Time-Dependent DFT (TDDFT)

In order to do calculation beyond the ground state, DFT need to be generalized onto the time-dependent domain. Runge, Gross and Sham did the generalization of the two Hohenberg-Kohn theorems, which set the theoretical foundation of TDDFT.

Consider a time-depend external electric field $V(t)$, and it is turned on at time when $t > t_0$,

$$V_{ext}(t) = \sum_{i=1}^{N} v_{ext}(\mathbf{r}_i, t). \tag{1.15}$$

Runge and Gross proved the Runge-Gross theorem that the wave functions for the many electron system can be determined by the electron density distribution ρ and a time dependent phase factor, i.e.

$$\Psi(t) = e^{-i\phi(t)}\Psi[\rho, \Psi_0](t), \tag{1.16}$$

where Ψ_0 is the initial wave function. Also, the electron density distribution ρ determines the external potential v_{ext} up to a time-dependent, space-independent factor

$c(t)$. Although Runge-Gross theorem suffers from some restriction[7] concerns about idealized systems, the real physical systems intended to model does not suffer from that. By assuming the initial state Ψ_0 is the ground state, Ψ_0 is determined by initial charge density $\rho(t = t_0)$. And the phase factor is canceled out when take the expectation value. The logic of TDDFT therefore is that by solving the electron density distribution in certain external field v_{ext}, the wave functions are implicitly determined as well as observables, i.e. $\rho(t) \to c(t) v_{ext}(t) \to e^{-i\phi(t)}\Psi(t) \to \mathcal{O}(t)$. Thus, by solving the time-dependent electron density distribution, the properties of the systems is obtained.

The generalization of second Hohenberg-Kohn theorem to time-dependent case is implemented by a variation principle on the action A, which is defined as

$$A = \int_{t_0}^{t_1} \langle \Psi(t) | i\frac{\partial}{\partial t} - H(t) | \Psi(t) \rangle dt. \tag{1.17}$$

The actual electron density distribution $\rho(\mathbf{r}, t)$ is the one that makes the action stationary:

$$\frac{\delta A}{\delta \rho(t)} = 0. \tag{1.18}$$

By using the same conception of reference state in DFT, the actual time-dependent system is mapped onto a fictitious system contains all independent electrons. We use $\psi_i(\mathbf{r}, t)$ to represent the wave function for the independent electron, which is also referred to as the molecular orbital, and use $\Psi(\mathbf{r}, t)$ to represent the total wave function which is a Slater determinant of $\{\psi_i(\mathbf{r}, t)\}$. The charge density $\rho(\mathbf{r}, t)$ is

$$\rho(\mathbf{r}, t) = \sum_{i}^{occ} |\psi_i(\mathbf{r}, t)|^2. \tag{1.19}$$

Defind A_{xc} as the difference of actions A for the actual system and for the reference system, i.e.

$$\begin{aligned} A_{xc}[\rho] = & \sum_i \int_{t_0}^{t_1} \langle \psi_i(\mathbf{r},t) | i\frac{\partial}{\partial t} - \frac{1}{2}\nabla^2 | \psi_i(\mathbf{r},t) \rangle \\ & - \frac{1}{2}\int_{t_0}^{t_1} \int\int \frac{\rho(\mathbf{r}_1,t)\,\rho(\mathbf{r}_2,t)}{|\mathbf{r}_1-\mathbf{r}_2|} d\mathbf{r}_1 d\mathbf{r}_2 dt \\ & - A[\rho] + \int_{t_0}^{t_1} \int v_{ext}(\mathbf{r},t)\,\rho(\mathbf{r},t)\,d\mathbf{r}dt. \end{aligned} \tag{1.20}$$

By doing the variation, the time-dependent Kohn-Sham equation is obtained as

$$-\frac{1}{2}\nabla^2\psi_i(\mathbf{r},t) + v_{ks}(\mathbf{r},t)\,\psi_i(\mathbf{r},t) = i\frac{\partial}{\partial t}\psi_i(\mathbf{r},t), \tag{1.21}$$

$$v_{ks}(\mathbf{r},t) = v_{ext} + v_{el} + \frac{\delta A_{xc}}{\delta\rho} = v_{ext}(\mathbf{r},t) + \int \frac{\rho(\mathbf{r},t)}{|\mathbf{r}-\mathbf{r}'|} d\mathbf{r}' + v_{xc}(\mathbf{r},t), \tag{1.22}$$

where A_{xc} is usually approximated by the time integration of exchange correlation energy E_{xc}

$$A_{xc} = \int_{t_0}^{t_1} E_{xc}[\rho(t)]\,dt. \tag{1.23}$$

1.4 Linear-Response TDDFT (LR-TDDFT)

On the top of Runge-Gross theorems as the foundation for TDDFT, one way of solving the time-dependent Kohn-Sham equation is by considering a weak external field as a perturbation to cause a linear response. Then by Fourier transform, the response function is transformed into the frequency domain, so that whether or not the system can be excited at a certain frequency of perturbation can be studied. This scheme of approach is the linear-response TDDFT (LR-TDDFT). Since it is the most widely used scheme and has implemented in most standard quantum chemistry codes, it is usually referred as the TDDFT calculation directly.

Denote $F_{pq}^{(0)}$ as the ground state Fock matrix element, i.e. the initial Fock matrix element, f_{pq} as the change of the corresponding Fock matrix element caused by the perturbation field, $P_{pq}^{(0)}$ as the ground state density matrix element i.e. the initial density matrix element, x_{ai} as the corresponding element represents the change in the occupied-virtual part density matrix, y_{ai} as the corresponding element represents the change in the virtual-occupied part density matrix, $\{i, j\}$ as the occupied Kohn-Sham orbitals, $\{a, b\}$ as the virtual (unoccupied) Kohn-Sham orbitals, and $\{p, q\}$ as any Kohn-Sham orbital regardless if it is occupied or virtual.

In LR-TDDFT, the response function finally has the form as[10]

$$F_{aa}^{(0)}x_{ai} - x_{ai}F_{ii}^{(0)} + \left(f_{ai} + \sum_{bj}\left\{\frac{\partial F_{ai}}{\partial P_{bj}}x_{bj} + \frac{\partial F_{ai}}{\partial P_{jb}}y_{bj}\right\}\right)P_{ii}^{(0)} = \omega x_{ai}, \tag{1.24}$$

$$F_{ii}^{(0)}y_{ai} - y_{ai}F_{aa}^{(0)} - P_{ii}^{(0)}\left(f_{ia} + \sum_{bj}\left\{\frac{\partial F_{ia}}{\partial P_{bj}}x_{bj} + \frac{\partial F_{ia}}{\partial P_{jb}}y_{bj}\right\}\right) = \omega y_{ai}. \tag{1.25}$$

Furthermore, it can be combined into one matrix equation

$$\begin{bmatrix}\mathbf{A} & \mathbf{B}\\ \mathbf{B}^* & \mathbf{A}^*\end{bmatrix}\begin{bmatrix}\mathbf{X}\\ \mathbf{Y}\end{bmatrix} = \omega\begin{bmatrix}\mathbb{I} & 0\\ 0 & -\mathbb{I}\end{bmatrix}\begin{bmatrix}\mathbf{X}\\ \mathbf{Y}\end{bmatrix}, \tag{1.26}$$

where $\mathbf{X} = \{x_{ai}\}$, $\mathbf{Y} = \{y_{ai}\}$, and

$$\mathbf{A}_{ia,jb} = \delta_{ij}\delta ab\left(\epsilon_a - \epsilon_b\right) + (ia|jb) + (ia|f_{xc}|jb)\,, \tag{1.27}$$

$$\mathbf{B}_{ia,jb} = (ia|jb) + (ia|f_{xc}|jb)\,. \tag{1.28}$$

f_{xc} is the xc kernel that

$$(ia|f_{xc}|jb) = \int \mathrm{d^3r d^3r'}\phi_{\mathrm{i}}^*(\mathrm{r})\phi_{\mathrm{a}}(\mathrm{r})\frac{\delta^2\mathrm{E_{xc}}}{\delta\rho(\mathrm{r})\delta\rho(\mathrm{r'})}\phi_{\mathrm{b}}^*(\mathrm{r'})\phi_{\mathrm{j}}(\mathrm{r'}). \tag{1.29}$$

To note here, $\mathbf{X}$, $\mathbf{Y}$ are column vectors , and either of them has the dimension of OV, where O is the number of occupied KS orbitals and V is the number of virtual orbitals. $\mathbf{A}$, $\mathbf{B}$ are both OV by OV square matrix.

According to Tamm-Dancoff approximation (TDA) [15], which is usually a good approximation in TDDFT calculation, the matrix $\mathbf{B}$ can be neglected, so that eq 1.26 finally is now simplified into an eigenvalue problem

$$\mathbf{AX} = \omega\mathbf{X}. \tag{1.30}$$

By solving eigenvalues and eigenvectors of matrix $\mathbf{A}$, excitation energies and excitation states are therefore obtained accordingly.

1.5 The Trade-Off Between CPU Time and Storage

The computation of electronic structure is restricted by the limited CPU ability and the limited hard-drive storage. If the algorithm required large amount of calculation, it may take too long the time for CPU to compute so that makes the calculation unrealistic. Or if the storage requirement is too high, for example, the matrix to store electronic information for a molecular system could be huge, the necessary initial, intermediate, or final data cannot be stored so that makes the algorithm invalid.

In the LR-TDDFT calculation, the major bottleneck is brought by the storage of matrix $\mathbf{A}$ and eigenvectors $\mathbf{X}$. To solve eq 1.30, Davidson iteration, which is a method to solve eigenvalues ω and corresponding eigenvector $\mathbf{X}$ iteratively from the lower eigenvalue state to the higher ones, is generally implemented, and the CPU cost

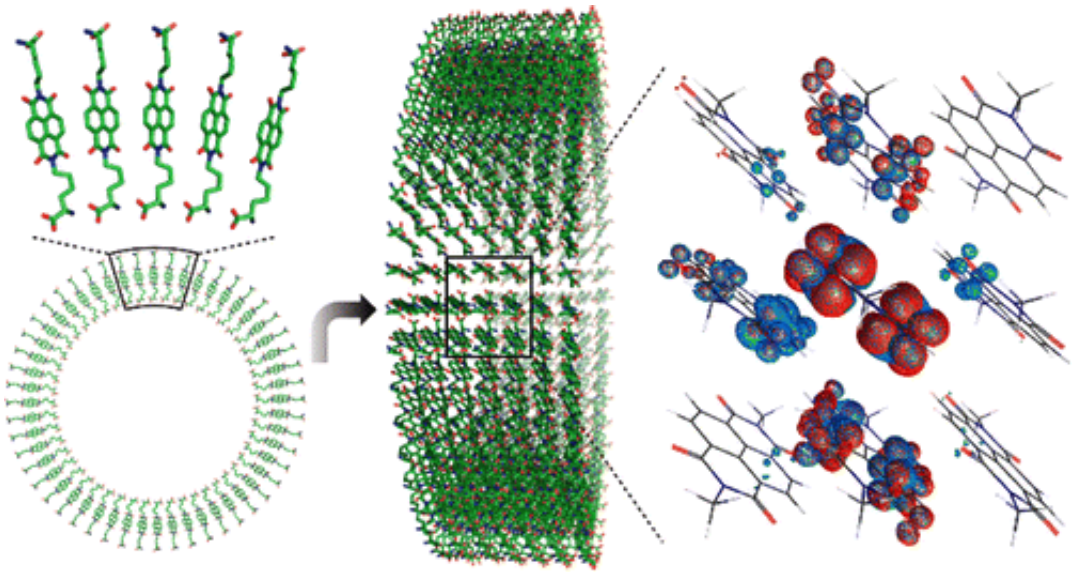

Figure 1.1: Semiconductor nanotube of naphthalene diimide (NDI) . Figure is from Ref. [2]. The LR-TDDFT calculation of such large structure is prohibitive by the limitation of storage. For a simplified model as $(NDI)_9$ on the right, the first bright state shown is already the 28th excited state.

for a few low-lying excited states is low. That makes LR-TDDFT a good candidate to calculate for small, or median sized molecular system, when aims at the first few excited states. However, the storage requirement due to the high dimension of $\mathbf{A}$, i.e. $\mathcal{O}(n^4)$ (proportional to the fourth of system size n), and $\mathbf{X}$, i.e. $\mathcal{O}(n^2)$ (proportional to the second of system size n), prohibits LR-TDDFT calculation for large systems or for seeking high energy states.

For example, in the calculation of a semiconductor nanotube which is composed of naphthalene diimide (NDI) monomers[2] (as in Figure 1.1), the system is too large so that only 9 NDI (as the right side of Figure 1.1) is calculated by LR-TDDFT with

a samll basis set 3-21+G*. Due to the high density of states, only one bright state is found during the computing until reaching the storage limit, and that state is already the 28th excited state. Because of the storage limitation and the dense density of states, higher bright states for the system are prohibitive to reach by LR-TDDFT.

For RT-TDDFT, one the contrary, the bottleneck is the high CPU cost. The detail of algorithms for RT-TDDFT calculation shows in the next chapter. RT-TDDFT is computed step-by-step in real-time. For each time step, the Fock matrix is reconstructed at least once by using the current external field and electron density distribution. The size for each time step should be comparatively small according to the electron movement. And the total time interval computed should be long enough to gather valid information on how a system response due to a certain perturbation. The Fock matrix keep its dimension ($\mathcal{O}(n^2)$) the same as that in the ground state DFT calculation. The CPU cost for each rebuild is approximately the same as each self-consistent-field (SCF) calculation. Therefore, the storage demand is no larger than that of the ground state calculation, and the entire CPU cost is about $N_{step} \times \Delta t_{SCF}$, where N_{step} is the total time steps, and Δt_{SCF} is the CPU cost per SCF calculation. In this case, although there is no worries on the storage limitation, the N_{step} is often large. When a large molecule system is calculated, Δt_{SCF} is also large. Thus, the total cost of CPU $N_{step} \times \Delta t_{SCF}$ can be so huge that the calculation requires months and years to run.

CHAPTER 2

Real-Time Time-Dependent Density Functional Theory

2.1 Equation of Motion

In the Real-Time approach of TDDFT, the property is calculated by the time dependent density matrix, which is obtained by direct integration over time. Start with the Kohn-Sham equation (eq 1.21 with 1.22),

$$-\frac{1}{2}\nabla^2\psi_i(\mathbf{r},t)+v_{ks}(\mathbf{r},t)\,\psi_i(\mathbf{r},t)=i\frac{\partial}{\partial t}\psi_i(\mathbf{r},t),$$

where

$$v_{ks}(\mathbf{r},t)=v_{ext}+v_{el}+\frac{\delta A_{xc}}{\delta\rho}=v_{ext}(\mathbf{r},t)+\int\frac{\rho(\mathbf{r},t)}{|\mathbf{r}-\mathbf{r}'|}\,\mathrm{d}\mathbf{r}'+\mathrm{v_{xc}}(\mathbf{r},\mathrm{t}).$$

Denote Fock operator $\mathbf{f}_{ks}$ as

$$\mathbf{f}_{ks}=-\frac{1}{2}\nabla^2+v_{ext}(\mathbf{r},t)+v_{el}(\mathbf{r},t)+v_{xc}(\mathbf{r},t). \tag{2.1}$$

So the Kohn-Sham equation becomes

$$i\frac{\partial}{\partial t}\psi_i(\mathbf{r},t)=\mathbf{f}_{ks}\psi_i(\mathbf{r},t). \tag{2.2}$$

We expand the time-dependent wave functions $\psi_i(\mathbf{r},t)$ into a static fixed basis with time varying coefficients. The fixed basis set is set as the ground state Kohn-Sham

orbitals, i.e. the molecular orbitals (MO) $\{\psi_i(\mathbf{r})\}$ obtained from the DFT ground state calculation. To be more computationally efficient, the orthogonal MO $\{\psi_i(\mathbf{r})\}$ are actual transferred into an orthogonal atomic orbital (AO) basis $\{\phi_\mu(\mathbf{r})\}$, which is an atom-centered Gaussian-function-like basis. The time-dependent wave function in the AO basis becomes

$$\psi_i(\mathbf{r},t) = \sum_{\mu=1}^{N_{AO}} C_{\mu i}(t)\,\phi_\mu(\mathbf{r}), \tag{2.3}$$

where $C_{\mu i}(t)$ is the time varying coefficient that can be represented as an element in the coefficient matrix $\mathbf{C}$. We denote N_{AO} as the number of atomic orbitals, N_{MO} as the number of molecular orbitals, and N_{occ} as the number of occupied molecular orbitals.

Consider the electron density distribution that

$$\begin{aligned}\rho(\mathbf{r}) = \sum_{i}^{N_{MO}} |\psi_i(\mathbf{r})|^2 &= \sum_{i}^{N_{MO}}\sum_{\mu}^{N_{AO}}\sum_{\nu}^{N_{AO}} \phi_\mu^*(\mathbf{r})\,C_{\mu i}^*(t)\,C_{\nu i}(t)\,\phi_\nu(\mathbf{r}) \\ &= \sum_{\mu}^{N_{AO}}\sum_{\nu}^{N_{AO}} \phi_\mu^*(\mathbf{r}) \left[\sum_{i}^{N_{MO}} C_{\nu i}(t)\,C_{\mu i}^*(t)\right]\phi_\nu(\mathbf{r}).\end{aligned} \tag{2.4}$$

We define the quantity in the square bracket as the element of the density matrix $\mathbf{P}$ that

$$\begin{aligned}&P_{\nu\mu} = \sum_{i}^{N_{MO}} C_{\nu i}(t)\,C_{\mu i}^*(t) = \sum_{i}^{N_{MO}} C_{\nu i}(t)\,C_{i\mu}^\dagger(t), \\ &\mathbf{P} = \mathbf{C}\mathbf{C}^\dagger.\end{aligned} \tag{2.5}$$

Define the overlap matrix $\mathbf{S}$ with its elements

$$S_{\mu\nu} = \int \phi_\mu^*(\mathbf{r})\,\phi_\nu(\mathbf{r})\,d\mathbf{r}. \tag{2.6}$$

Define the Fock Matrix $\mathbf{F}$ with its elements

$$F_{\mu\nu}\left[\rho_t\right] = \langle\phi_\mu|\mathbf{f}_{ks}|\phi_\nu\rangle. \tag{2.7}$$

Therefore, the Kohn-Sham equation in AO basis set can be written as

$$i\frac{\partial}{\partial t}\sum_{\mu=1}^{N_{AO}} C_{\mu i}\left(t\right)\left|\phi_\mu\left(\mathbf{r}\right)\right\rangle = \mathbf{f}_{ks}\sum_{\mu=1}^{N_{AO}} C_{\mu i}\left(t\right)\left|\phi_\mu\left(\mathbf{r}\right)\right\rangle. \tag{2.8}$$

By multiplying both sides by $\langle\phi_\nu|$, the equation is simplified as

$$\begin{aligned}
\langle\phi_\nu|i\frac{\partial}{\partial t}\sum_{\mu=1}^{N_{AO}} C_{\mu i}\left(t\right)\left|\phi_\mu\right\rangle &= \langle\phi_\nu|\mathbf{f}_{ks}\sum_{\mu=1}^{N_{AO}} C_{\mu i}\left(t\right)\left|\phi_\mu\right\rangle, \\
i\sum_{\mu=1}^{N_{AO}}\langle\phi_\nu|\phi_\mu\rangle\frac{\partial}{\partial t}C_{\mu i}\left(t\right) &= \sum_{\mu=1}^{N_{AO}} C_{\mu i}\left(t\right)\langle\phi_\nu|\mathbf{f}_{ks}|\phi_\mu\rangle, \\
i\sum_{\mu=1}^{N_{AO}} S_{\nu\mu}\frac{\partial}{\partial t}C_{\mu i}\left(t\right) &= \sum_{\mu=1}^{N_{AO}} C_{\mu i}\left(t\right)F_{\nu\mu}.
\end{aligned} \tag{2.9}$$

Represent in the matrix form as

$$i\mathbf{S}\frac{\partial}{\partial t}\mathbf{C}\left(t\right) = \mathbf{FC}. \tag{2.10}$$

Take adjoint for both sides of eq 2.10 as

$$-i\frac{\partial}{\partial t}\mathbf{C}\left(t\right)^\dagger\mathbf{S}^\dagger = \mathbf{C}^\dagger\mathbf{F}^\dagger. \tag{2.11}$$

Multiply eq 2.10 right by $\mathbf{C}\left(t\right)^\dagger\mathbf{S}^\dagger$, and multiply eq 2.11 left by $\mathbf{SC}\left(t\right)$, which gives

$$i\mathbf{S}\frac{\partial}{\partial t}\mathbf{C}\left(t\right)\mathbf{C}\left(t\right)^\dagger\mathbf{S}^\dagger = \mathbf{FCC}\left(t\right)^\dagger\mathbf{S}^\dagger, \tag{2.12}$$

$$-i\mathbf{SC}\left(t\right)\frac{\partial}{\partial t}\mathbf{C}\left(t\right)^\dagger\mathbf{S}^\dagger = \mathbf{SC}\left(t\right)\mathbf{C}^\dagger\left(t\right)\mathbf{F}^\dagger. \tag{2.13}$$

Subtract eq 2.12 by eq 2.13, which gives

$$i\mathbf{S}\left(\mathbf{C}\frac{\partial}{\partial t}\mathbf{C}^{\dagger}+\frac{\partial}{\partial t}\mathbf{C}^{\dagger}\mathbf{C}\right)\mathbf{S}^{\dagger}=\mathbf{FCC}^{\dagger}\mathbf{S}^{\dagger}-\mathbf{SCC}^{\dagger}\mathbf{F}^{\dagger}. \tag{2.14}$$

By substituting with density matrix $\mathbf{P}$, the equation of motion in the AO basis is obtained as

$$i\mathbf{S}\left(\frac{\partial}{\partial t}\mathbf{P}\right)\mathbf{S}^{\dagger}=\mathbf{FPS}^{\dagger}-\mathbf{SPF}^{\dagger}. \tag{2.15}$$

We avoid using $\mathbf{S}^{-1}$ in the manipulation of matrix above to circumvent the problem caused by the existence of $\mathbf{S}^{-1}$.

2.2 Transformation of Basis

The overlap matrix $\mathbf{S}$ is a static matrix determined by the chosen AO basis set. $\mathbf{S}$ can be transformed into an identity matrix via a so-called Löwdin basis transformation, thereby the computation of eq 2.15 is greatly simplified.

Assume $\mathbf{s}$ is a diagonal matrix, whose diagonal elements are the eigenvalues of the overlap matrix $\mathbf{S}$, and the unitary matrix $\mathbf{U_s}$ is the corresponding transformation matrix, i.e.

$$\mathbf{U}_s^{\dagger}\,\mathbf{S}\,\mathbf{U}_s=\begin{pmatrix} s_1 & & & & \\ & s_2 & & & \\ & & s_3 & & \\ & & & \ddots & \\ & & & & s_n \end{pmatrix}=\mathbf{s}, \tag{2.16}$$

where $\mathbf{S}$ is a Hermitian matrix, and its eigenvalues are real and positive. Denote

diagonal matrix $\mathbf{s}^{\frac{1}{2}}$ with diagonal elements are the square root of that in $\mathbf{s}$, i.e.

$$\mathbf{s}^{\frac{1}{2}} = \begin{pmatrix} s_1^{\frac{1}{2}} & & & & \\ & s_2^{\frac{1}{2}} & & & \\ & & s_3^{\frac{1}{2}} & & \\ & & & \ddots & \\ & & & & s_n^{\frac{1}{2}} \end{pmatrix}. \tag{2.17}$$

Assume diagonal matrix $\mathbf{s}^{-\frac{1}{2}}$ whose diagonal terms are the inverse square root of corresponding terms in $\mathbf{s}$, i.e.

$$\mathbf{s}^{-\frac{1}{2}} = \begin{pmatrix} s_1^{-\frac{1}{2}} & & & & \\ & s_2^{-\frac{1}{2}} & & & \\ & & s_3^{-\frac{1}{2}} & & \\ & & & \ddots & \\ & & & & s_n^{-\frac{1}{2}} \end{pmatrix}. \tag{2.18}$$

Define the transformation $\mathbf{X}$ as

$$\mathbf{X} = \mathbf{U_s} \mathbf{s}^{-\frac{1}{2}}. \tag{2.19}$$

Transform the previous AO basis ϕ_ν into ϕ'_ν as

$$\phi'_\mu = \sum_\nu X_{\nu\mu} \phi_\nu. \tag{2.20}$$

Since it can be easily proved that

$$\mathbf{X}^\dagger \mathbf{S} \mathbf{X} = \mathbf{s}^{-\frac{1}{2}}\, \mathbf{U}_\mathbf{s}^\dagger\, \mathbf{S}\, \mathbf{U_s}\, \mathbf{s}^{-\frac{1}{2}} = \mathbb{I}, \tag{2.21}$$

and

$$\mathbf{S} = \left(\mathbf{X}^\dagger\right)^{-1} (\mathbf{X})^{-1}, \tag{2.22}$$

where $\mathbf{X}^{-1}$ is obtained from eq 2.19 that

$$\mathbf{X}^{-1} = \mathbf{s}^{\frac{1}{2}}\, \mathbf{U}_\mathbf{s}^\dagger. \tag{2.23}$$

Now we can simplify eq 2.15. Substitute $\mathbf{S}$, which gives,

$$\left(\mathbf{X}^{\dagger}\right)^{-1}\mathbf{X}^{-1}\left(\frac{\partial}{\partial t}\mathbf{P}\right)\left(\mathbf{X}^{\dagger}\right)^{-1}\mathbf{X}^{-1}=i\left(\mathbf{X}^{\dagger}\right)^{-1}\mathbf{X}^{-1}\mathbf{P}\,\mathbf{F}-\mathbf{F}\,\mathbf{P}\left(\mathbf{X}^{\dagger}\right)^{-1}\mathbf{X}^{-1}. \quad (2.24)$$

Left multiply $\mathbf{X}^{\dagger}$ the both sides and right multiply $\mathbf{X}$ the both sides, which gives,

$$\begin{aligned}
&\mathbf{X}^{-1}\left(\frac{\partial}{\partial t}\mathbf{P}\right)\left(\mathbf{X}^{\dagger}\right)^{-1}=i\mathbf{X}^{-1}\mathbf{P}\,\mathbf{F}\,\mathbf{X}-\mathbf{X}^{\dagger}\,\mathbf{F}\,\mathbf{P}\left(\mathbf{X}^{\dagger}\right)^{-1},\\
&\mathbf{X}^{-1}\left(\frac{\partial}{\partial t}\mathbf{P}\right)\left(\mathbf{X}^{\dagger}\right)^{-1}=i\mathbf{X}^{-1}\mathbf{P}\left[\left(\mathbf{X}^{\dagger}\right)^{-1}\mathbf{X}^{\dagger}\right]\mathbf{F}\,\mathbf{X}-\mathbf{X}^{\dagger}\,\mathbf{F}\left[\mathbf{X}\,\mathbf{X}^{-\mathbf{1}}\right]\mathbf{P}\left(\mathbf{X}^{\dagger}\right)^{-1},\\
&\frac{\partial}{\partial t}\left[\mathbf{X}^{-1}\mathbf{P}\left(\mathbf{X}^{\dagger}\right)^{-1}\right]=i\left[\mathbf{X}^{-1}\mathbf{P}\left(\mathbf{X}^{\dagger}\right)^{-1}\right]\left[\mathbf{X}^{\dagger}\,\mathbf{F}\,\mathbf{X}\right]-\left[\mathbf{X}^{\dagger}\,\mathbf{F}\,\mathbf{X}\right]\left[\mathbf{X}^{-\mathbf{1}}\mathbf{P}\left(\mathbf{X}^{\dagger}\right)^{-1}\right].
\end{aligned} \quad (2.25)$$

Denote $\mathbf{P}'$ and $\mathbf{F}'$ as

$$\mathbf{P}'=\mathbf{X}^{-1}\mathbf{P}\left(\mathbf{X}^{\dagger}\right)^{-1}, \quad (2.26)$$

$$\mathbf{F}'=\mathbf{X}^{\dagger}\,\mathbf{F}\,\mathbf{X}. \quad (2.27)$$

The equation of motion therefore is

$$\frac{\partial}{\partial t}\mathbf{P}'=i\left[\mathbf{P}'\mathbf{F}'-\mathbf{F}'\mathbf{P}'\right]=i\left[\mathbf{P}',\mathbf{F}'\right]. \quad (2.28)$$

Eq 2.28 is much more easier to be solved than the previous equation eq 2.15.

2.3 Time-Dependent Fock Matrix

The Fock matrix is time-varying and dependent on the density matrix $\mathbf{P}(t)$. In the below provides the explicit form for the Fock matrix computation. It is a summation over the one-electron part $H_{\mu\nu}$, the two-electron Coulomb interaction $G^{J}_{\mu\nu}[\mathbf{P}(t)]$,

the two-electron exchange-correlation $G_{\mu\nu}^{XC}\left[\mathbf{P}\left(t\right)\right]$, and the potential energy of time-dependent external field $\overrightarrow{D_{\mu\nu}}\cdot\overrightarrow{\mathbf{E}\left(t\right)}$.

$$\begin{aligned}
F_{\mu\nu}\left[\rho_t\right] &= \langle\phi_\mu|\mathbf{f}_{ks}|\phi_\nu\rangle = \langle\phi_\mu|-\frac{1}{2}\nabla^2+v_{ext}\left(\mathbf{r},t\right)+v_{el}\left(\mathbf{r},t\right)+v_{xc}\left(\mathbf{r},t\right)|\phi_\nu\rangle,\\
&= \langle\phi_\mu|-\frac{1}{2}\nabla^2|\phi_\nu\rangle+\langle\phi_\mu|v_{el}\left(\mathbf{r},t\right)|\phi_\nu\rangle+\langle\phi_\mu|v_{xc}\left(\mathbf{r},t\right)|\phi_\nu\rangle+\langle\phi_\mu|v_{ext}\left(\mathbf{r},t\right)|\phi_\nu\rangle,\\
&= H_{\mu\nu}+G_{\mu\nu}^{J}\left[\mathbf{P}\left(t\right)\right]+G_{\mu\nu}^{XC}\left[\mathbf{P}\left(t\right)\right]+D_{\mu\nu}^{x}\cdot E_x\left(t\right)+D_{\mu\nu}^{y}\cdot E_y\left(t\right)+D_{\mu\nu}^{z}\cdot E_z\left(t\right),\\
&= H_{\mu\nu}+G_{\mu\nu}^{J}\left[\mathbf{P}\left(t\right)\right]+G_{\mu\nu}^{XC}\left[\mathbf{P}\left(t\right)\right]+\overrightarrow{D_{\mu\nu}}\cdot\overrightarrow{\mathbf{E}\left(t\right)}.
\end{aligned} \tag{2.29}$$

$\overrightarrow{\mathbf{D}}$ is the dipole matrix $\overrightarrow{\mathbf{D}}=(\mathbf{D}^x,\mathbf{D}^y,\mathbf{D}^z)$, and $D^{\alpha}{}_{\mu\nu}=\langle\phi_\mu|\alpha|\phi_\nu\rangle$, with $\alpha=x,y,z$. By using eq 2.27,

$$\begin{aligned}
\mathbf{F}' &= \mathbf{X}^\dagger\,\mathbf{F}\,\mathbf{X},\\
&= \mathbf{X}^\dagger\,H_{\mu\nu}\,\mathbf{X}+\mathbf{X}^\dagger\,G_{\mu\nu}^{J}\left[\mathbf{P}\left(t\right)\right]\,\mathbf{X}+\mathbf{X}^\dagger\,G_{\mu\nu}^{XC}\left[\mathbf{P}\left(t\right)\right]\,\mathbf{X}+\mathbf{X}^\dagger\,\overrightarrow{D_{\mu\nu}}\,\mathbf{X}\cdot\overrightarrow{\mathbf{E}\left(t\right)},\\
&= H'_{\mu\nu}+G'^{J}_{\mu\nu}\left[\mathbf{P}\left(t\right)\right]+G'^{XC}_{\mu\nu}\left[\mathbf{P}\left(t\right)\right]+\overrightarrow{D'_{\mu\nu}}\cdot\overrightarrow{\mathbf{E}\left(t\right)}.
\end{aligned} \tag{2.30}$$

To note here, in the calculation of $\mathbf{F}'$, the one-electron part $H'_{\mu\nu}$ is time-independent, the two-electron parts $G'^{J}_{\mu\nu}\left[\mathbf{P}\left(t\right)\right]$ and $G'^{XC}_{\mu\nu}\left[\mathbf{P}\left(t\right)\right]$ both depend on time-dependent density matrix $\mathbf{P}\left(t\right)$, and the last term depends on time varying external field $\overrightarrow{\mathbf{E}\left(t\right)}$.

2.4 Propagator

The solution of eq 2.28 has the form as

$$\mathbf{P}'\left(t\right)=\mathbf{U}\left(t,t_0\right)\mathbf{P}'\left(t_0\right)\mathbf{U}^\dagger\left(t,t_0\right), \tag{2.31}$$

where $\mathbf{U}\left(\tau,\mathbf{t}\right)$ is the propagator that

$$\mathbf{U}\left(t,t_0\right)=\mathcal{T}\exp\left[\int_{t_0}^{t}-i\mathbf{F}'_\tau\mathrm{d}\tau\right]. \tag{2.32}$$

$\mathcal{T}$ is the time ordering operator, which means

$$\mathcal{T}\exp\left[\int_{t_0}^{t}-i\mathbf{F}'_{\tau}\mathrm{d}\tau\right]=\lim_{\delta t\to 0}\left\{\left[\exp\left(i\mathbf{F}'_{t}\delta t\right)\right]\left[\exp\left(i\mathbf{F}'_{t-\delta t}\delta t\right)\right]\left[\exp\left(i\mathbf{F}'_{t-2\delta t}\delta t\right)\right]\right.$$
$$\left.\cdots\left[\exp\left(i\mathbf{F}'_{t_0+\delta t}\delta t\right)\right]\left[\exp\left(i\mathbf{F}'_{t_0}\delta t\right)\right]\right\}. \tag{2.33}$$

The time ordering operator is not unnecessary, for the reason that $\mathbf{F}'_{\tau}$ at different time τ are not necessarily interchangeable (i.e. not commute). The natural approach to approximate propagator $\mathbf{U}(t,t_0)$ is to divide the total time interval into small sub-intervals as time-steps and update density matrix $\mathbf{P}$ by each time step. Assume the total time interval, i.e. the propagation duration, is T and separate it into n equal sub-interval Δt. The propagator can be represented as the multiplication of N propagators as

$$\mathbf{U}(t,t_0)\approx\prod_{n=0}^{N-1}\mathbf{U}\left((n+1)\Delta t,n\Delta t\right), \tag{2.34}$$

with

$$\mathbf{U}\left((n+1)\Delta t,n\Delta t\right)=\mathcal{T}\exp\int_{n\Delta t}^{(n+1)\Delta t}[-i\mathbf{F}'_{\tau}\mathrm{d}\tau], \tag{2.35}$$

and the density matrix $\mathbf{P}'$ is updated as

$$\mathbf{P}'(\tau+\Delta t)=\mathbf{U}(\tau+\Delta t,\tau)\ \mathbf{P}'(\tau)\ \mathbf{U}^{\dagger}(\tau+\Delta t,\tau). \tag{2.36}$$

Therefore, the time-ordering integration for a small interval can be approximated by algorithms.

The algorithms to approximate the propagator contains two parts. The first part is how to approximate the time-ordering integration. And the second part is the calculation of matrix exponentiation.

2.4.1 Algorithms for the Time-Ordering Integration

The time-ordering integration need to be done numerically. To start with, Fock matrix $F(\tau)$ at different time, such as $F(\tau_1)$, $F(\tau_2)$, are not necessary commute with each other, so the integration of the exponent can not be simply analytically done. Meanwhile, the calculation of integration for the propagator $U((n+1)\Delta t, n\Delta t)$ requires knowledge of the future information on the Fock matrix. However, the future Fock matrix can only be roughly guessed.

To solve this, algorithms are designed to reach the self-consistency between the extrapolation value and the interpolation value[16]. But once the time step is taken too large, the prediction of the Future Fock Matrix is easily failed. Ideally, we would like propagator calculated every step with the consistency for the Fock matrix.

Denote $\mathbf{A}(\tau) = -i\mathbf{F}'_\tau$. The steps to reach a self-consistent propagation is as follow:

(1). obtain $\mathbf{F}'_t$ at the future time t by extrapolation;

(2). propagate $\mathbf{P}'(\tau)$ from the current time τ, onto $\mathbf{P}'(\tau + \Delta t)$ at the next time step $\tau + \Delta t$;

(3). calculate $\mathbf{F}'_{\tau+\Delta t}$ by using $\mathbf{P}'(\tau + \Delta t)$ from the last step, and get $\mathbf{F}'_t$ by interpolating between $\mathbf{F}'_{\tau+\Delta t}$ and $\mathbf{F}'_\tau$;

(4). compare the $\mathbf{F}'_t$ from the step (3) and the $\mathbf{F}'_t$ from the step (1); repeat the process until reach the self-consistency.

If assume the Fock matrix can be obtained exactly via the steps above, the algorithms to calculate the propagator are as follow.

Exponential Midpoint Rule

The exponential midpoint (EM) rule approximate the propagator by using $\mathbf{F}'_t$ at the mid-point of the time step, i.e.

$$\mathbf{U}\left(t+\Delta t\right)=\exp\left[-i\Delta\mathbf{F}'_{t+\Delta t/2}\right]. \tag{2.37}$$

Enforced Time-Reversal Symmetry Methods

Enforced time-reversal symmetry methods (ETRS) enforces the propagator to have the time-reversal symmetry by using the simplest propagator approximation

$$\exp\left[i\mathbf{F}'_{t+\Delta t}\frac{\Delta t}{2}\right]\phi\left(t+\Delta t\right)=\exp\left[-i\mathbf{F}'_{t}\frac{\Delta t}{2}\right]\phi\left(t\right). \tag{2.38}$$

This leads to the propagator as

$$\mathbf{U}_{ETRS}\left(t+\Delta t,t\right)=\exp\left[-i\mathbf{F}'_{t+\Delta t}\frac{\Delta t}{2}\right]\times\exp\left[-i\mathbf{F}'_{t}\frac{\Delta t}{2}\right]. \tag{2.39}$$

Implicit Midpoint Rule

Implicit midpoint (IM) propagator is obtained by simplest approximation the propagator at the mid-point. The expansion is up to the first order to enforce the time-reversal symmetry.

$$\begin{aligned}
&\mathbf{U}\left(t+\Delta t/2,t+\Delta t\right)\phi\left(t+\Delta t\right)=\mathbf{U}\left(t+\Delta t/2,t\right)\phi\left(t\right),\\
&\exp\left[i\mathbf{F}'_{t+\Delta t/2}\frac{\Delta t}{2}\right]\phi\left(t+\Delta t\right)=\exp\left[-i\mathbf{F}'_{t+\Delta t/2}\frac{\Delta t}{2}\right]\phi\left(t\right),\\
&\left[\mathbb{I}+i\mathbf{F}'_{t+\Delta t/2}\frac{\Delta t}{2}\right]\phi\left(t+\Delta t\right)=\left[\mathbb{I}-i\mathbf{F}'_{t+\Delta t/2}\frac{\Delta t}{2}\right]\phi\left(t\right).
\end{aligned} \tag{2.40}$$

$$\mathbf{U}_{IM}\left(t+\Delta t,t\right)=\frac{\mathbb{I}-i\mathbf{F}'_{t+\Delta t/2}\frac{\Delta t}{2}}{\mathbb{I}+i\mathbf{F}'_{t+\Delta t/2}\frac{\Delta t}{2}}. \tag{2.41}$$

Magnus expansion

For the exponential integration problem like $\exp \int_{\tau} \mathbf{A}(\tau)\, d\tau$, it is mathematical proved that it can be expanded using Magnus expansion. i.e.

$$\begin{aligned}
&\mathcal{T} \exp \int_0^t A(t)\, dt = e^{\Omega_1+\Omega_2+\Omega_3+\cdots}, \\
&\Omega_1(t) = \int_0^t A(\tau_1)\, d\tau_1, \\
&\Omega_2(t) = \frac{1}{2} \int_0^t d\tau_1 \int_0^{\tau_1} \tau_2 \left[A(\tau_1), A(\tau_2)\right], \\
&\Omega_3(t) = \frac{1}{6} \int_0^t d\tau_1 \int_0^{\tau_1} \tau_2 \int_0^{\tau_2} d\tau_3 \left(\left[A(\tau_1), \left[A(\tau_2), A(\tau_3)\right]\right] + \left[A(\tau_3), \left[A(\tau_2), A(\tau_1)\right]\right]\right).
\end{aligned} \tag{2.42}$$

By using the 1^{st} order Magnus expansion, we actually get a propagator the same as the mid-point rule, i.e.

$$\begin{aligned}
&\mathbf{U}(t+\Delta t, t) \approx e^{\Omega_1}, \\
&\Omega_1 \approx -i\mathbf{F}_{t+\frac{\Delta t}{2}} \Delta t.
\end{aligned} \tag{2.43}$$

To note here, the higher the order of the expansion, the more accurate the propagator is obtained, and the larger the time interval can be take. Since the high cost of RT-TDDFT calculation is mainly due to the large number of times of building Fock matrix, it is natural to lower the cost by enlarge the size for each time step. However, as the size of the time step is increasing, the order of magnus expansion is increasing accordingly to make sure for a valid Fock matrix. Therefore the number of times of building Fock matrix for each interval is also increasing. But the Fock matrix in the future time is obtained by a rough prediction that could be easily failed if the size of the time step is too large. Also, the overall numbers of times of building the Fock

matrix can still be large when the self-consistent propagator is hard to converge with the large time step. So it is not always better by using a larger time-step or a higher order expansion.

2.4.2 Algorithms for the Matrix Exponentiation

The algorithm need be able to be accurate and efficient. Since the same exponentiation algorithm is used for calculations at each time step, any inaccuracy of the algorithm builds up as calculation goes. In this section, we use matrix $\mathbf{A}$ to represent the exponent.

Tylor Expansion

The exponentiation of the matrix is defined by Tylor expansion:

$$\exp(\mathbf{A}) = \sum_{n=0}^{\infty} \left(\frac{1}{n!} \mathbf{A}^n \right). \tag{2.44}$$

Tylor expansion can be used to approximate $\exp(\mathbf{A})$ to a certain order. But this method is not preferred for the reason that the propagator can lose its unitarity easily if the approximation order is small, while the efficiency is low if the order is high.

Unitary Transformation

By considering the fact that $\mathbf{F}'_\tau$ is always the hermitian matrix, $\mathbf{F}'_\tau$ can be diagonalized by a unitary transformation[17] $\mathbf{U}_F$ at any time τ. $\mathbf{A}(\tau) = -i\mathbf{F}'_\tau$ can also be

diagonalized by $\mathbf{U}_F$. Therefore, $\exp(\mathbf{A})$ can be exactly calculated as

$$\begin{aligned}\exp(\mathbf{A}) &= \sum_{n=0}^{\infty} \frac{1}{n!} \mathbf{A}^n \\ &= \left(\mathbf{U_F U_F^\dagger}\right) \sum_{n=0}^{\infty} \frac{1}{n!} \mathbf{A}^n \left(\mathbf{U_F U_F^\dagger}\right) \\ &= \mathbf{U_F} \left\{ \sum_{n=0}^{\infty} \frac{1}{n!} \left[\mathbf{U_F^\dagger A U_F}\right]^n \right\} \mathbf{U_F^\dagger} \\ &= \mathbf{U_F} \exp\left(\mathbf{U_F^\dagger A U_F}\right) \mathbf{U_F^\dagger}.\end{aligned} \tag{2.45}$$

Since $\mathbf{U_F^\dagger A U_F}$ is an diagonal matrix, each of the diagonal elements can be exactly calculated by exponentiation. $\mathbf{F}'_\tau$ is time-dependent, so $\mathbf{F}'_\tau$ need to be diagonalized and obtain the corresponding $\mathbf{U}_F$ for each of time steps.

Baker-Campbell-Hausdorff Formula

Baker-Campbell-Hausdorff (BCH) expansion is another expansion method[14]. If a calculation in the form as

$$\mathbf{P'}(t + \Delta t) = e^{\mathbf{A}} \mathbf{P'}(t)\, e^{-\mathbf{A}}, \tag{2.46}$$

it can be expended by BCH formula as

$$\begin{aligned}\mathbf{P'}(t + \Delta t) = \mathbf{P'}(t) &+ \frac{1}{1!}[\mathbf{A}, \mathbf{P'}(t)] + \frac{1}{2!}[\mathbf{A}, [\mathbf{A}, \mathbf{P'}(t)]] \\ &+ \frac{1}{3!}[\mathbf{A}, [\mathbf{A}, [\mathbf{A}, \mathbf{P'}(t)]]] + \cdots .\end{aligned} \tag{2.47}$$

By choosing different orders of the BCH expansion, different accuracy can be obtained.

Besides all algorithm listed above, there are other approximations, such as Chebychev polynomial expansion, Krylov subspace projection, etc.

CHAPTER 3

Results by RT-TDDFT calculation in the Regime of Linear Optical Response

3.1 Linear Optical Response

For a multi-electron system in the external electric field $\mathbf{E} = (E_x, E_y, E_z)$, the time-dependent dipole moment has the expansion as

$$\begin{aligned} p_i(t) &= p_{i0} + \sum_j \int_{-\infty}^{\infty} \alpha_{ij}(t-\tau_1) E_j(\tau_1)\, d\tau_1 \\ &+ \sum_{jk} \int_{-\infty}^{\infty}\int_{-\infty}^{\infty} \beta_{ijk}(t-\tau_1, t-\tau_2) E_j(\tau_1) E_k(\tau_2)\, d\tau_1\, d\tau_2 \\ &+ \sum_{jkl} \int_{-\infty}^{\infty}\int_{-\infty}^{\infty}\int_{-\infty}^{\infty} \gamma_{ijkl}(t-\tau_1, t-\tau_2, t-\tau_3) E_j(\tau_1) E_k(\tau_2) E_l(\tau_3)\, d\tau_1\, d\tau_2\, d\tau_3 \cdots . \end{aligned} \tag{3.1}$$

p_i is the dipole moment in direction i, p_{i0} is the permanent dipole moment in direction i, where $i, j, k = x, y, z$. α_{ij} is the linear polarizability. β_{ijk}, γ_{ijkl}, $\cdots$ are the higher order polarizability. In the weak field limit, linear response is dominating the change of dipole moment δp. Therefore, we only consider α as polarizability tensor. α_{ij} represents the polarizability at i direction while electric field in j direction. The change of the time-dependent dipole moment is the integration of dynamic polarizability and

electric field, i.e.

$$\delta p_i(t) \approx \sum_j \int_{-\infty}^{\infty} \alpha_{ij}(t-\tau_1) E_j(\tau_1)\, d\tau_1. \tag{3.2}$$

By the convolution theorem, the Fourier transform of α_{ij} is

$$\alpha_{ij}(\omega) = \frac{\delta p_i(\omega)}{E_j(\omega)}. \tag{3.3}$$

The absorption cross-section tensor is[14]

$$\sigma(\omega) = \frac{4\pi\omega}{c} Im[\alpha(\omega)]. \tag{3.4}$$

the dipole absorption spectrum, i.e. the dipole strength function, is

$$S(\omega) = \frac{1}{3} Tr[\sigma(\omega)]. \tag{3.5}$$

Since the trace is invariant under unitary transformation, the spectrum $S(\omega)$ is independent of the direction of the molecule.

In the real-time calculation, the system in ground state is excited by a δ-function-like (in the time domain) electric field, by which a wide range of energy states can be excited. Some excited states are prohibited during excitation by the symmetry. They are called as dark states. The probabilities of transition for them are very close to zero, i.e. $\mathcal{P}_{n0} \propto |\langle n|\widehat{\mathbf{d}}|0\rangle|^2 \approx 0$. During and after the excitation, The initial system evolves into a superposition of excited states, and each of these excited state is oscillating with the frequency corresponding to its excitation energy. The total dipole moment of the system therefore oscillates. By Fourier analysis the time-varying dipole moment, the energies of excited states are revealed.

3.2 The Comparison of Results Between RT-TDDFT and LR-TDDFT Calculation

The initial state of the system is the ground state calculated by DFT. Then the system is excited by a δ-function-like electric field $E(t)$ shown as below and propagates over time.

$$\overrightarrow{E(t)} = E_0 \exp\left[\frac{-(t-t_0)^2}{2w^2}\right]\widehat{e}. \tag{3.6}$$

E_0 is the maximum field strength. $\widehat{e}$ is the direction of the electric field. The width of the excitation pulse is determined by ω. The calculation of RT-TDDFT is done by using the pilot codes[1] in Q-Chem quantum chemistry calculation package. The codes use a simple implementation of mid-point algorithm (2.4.1 mid-point) without keeping the extrapolation interpolation self-consistency. The exponential is calculated by using unitary transformation (2.4.2 unitary transformation). The results of RT-TDDFT calculation should agree with the results of LR-TDDFT calculation when the external field is weak, i.e. when E_0 is small. The calculation of LR-TDDFT to be compared with is done by using the well-constructed codes in Q-Chem.

3.2.1 CH_4 molecule

In the calculation for CH_4, time step $\Delta t = 0.02$ a.u., electric field $t_0 = 0.49$ a.u. , $w = 0.07$ a.u., $E_0 = 0.001$ a.u.. The basis is 6-31G*, and the functional is ω-pbe for both RT and LR calculation. The first 24 excited states obtained form LR-TDDFT is calculated. The dipole moment changing with time is shown in figure 3.1. After the excitation by a delta-function like electric field (lines in red), the dipole moment

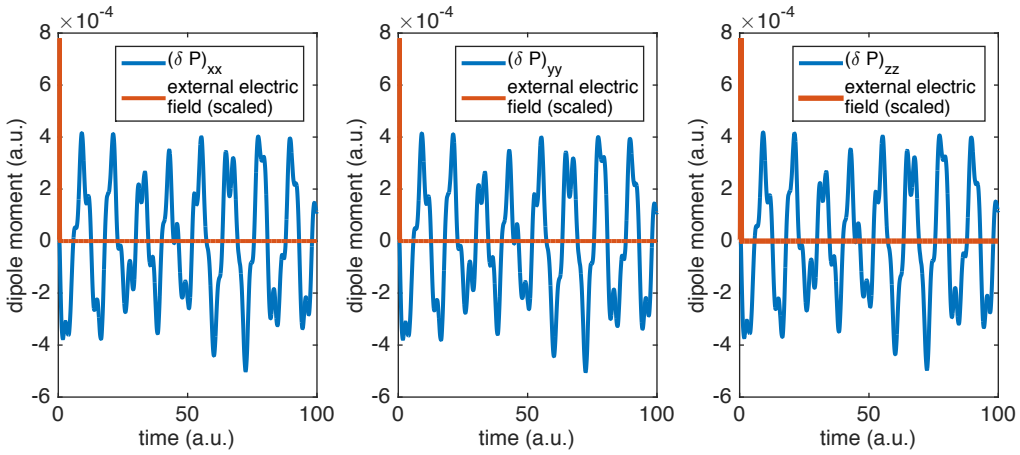

Figure 3.1: The response of dipole moment for CH_4 in real-time. After the excitation by a delta-function like electric field (lines in red), the dipole moment oscillates. δP_{ii}, where $i = x, y, z$, represents the change of dipole moment at i direction due to the electric field in i direction.

oscillates. δP_{ii}, where $i = x, y, z$, represents the change of dipole moment at i direction due to the electric field in i direction. As in figure 3.1, the change of dipole moment in different directions over time are almost identical. This is because of the symmetry of CH_4 molecule.

The bright states for CH_4 calculated by RT-TDDFT have a very good agreement with that of LR-TDDFT, as shown in the upper graph of figure 3.2. The difference between the spectrum peak by RT-TDDFT calculation and the corresponding excitation energy by LR-TDDFT calculation is within 0.3 eV for all bright states. In the lower graph of figure 3.2, we compare the spectrum generated by using different total time integration intervals. When the total time interval is short, the peaks of spectrum is broad, and the peak is not accurately converged at the correct value. As

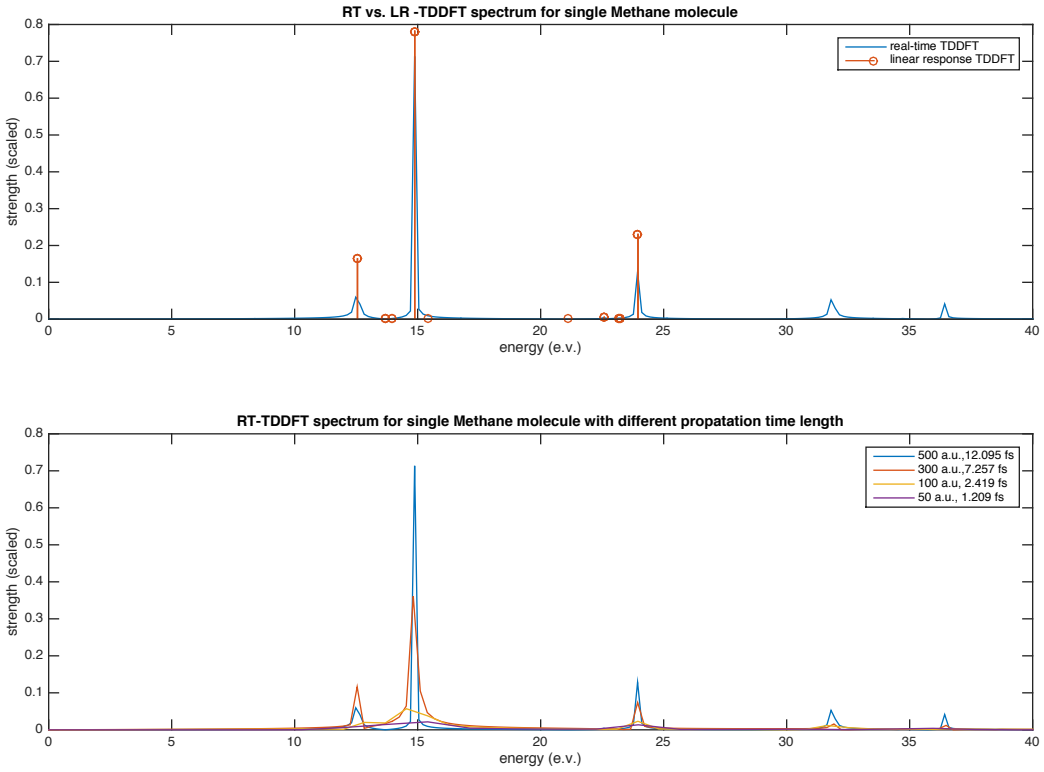

Figure 3.2: Comparison between RT-TDDFT results and LR-TDDFT results for CH_4. In the upper graph, The bright states for CH_4 calculated by RT-TDDFT have a very good agreement with that of LR-TDDFT. In the lower graph, we compare the spectrum generated by using different total time integration intervals. As the total time interval being larger, peaks are narrower, higher, and converged to the correct values.

the total time interval being larger, peaks are narrower, higher, and converged to the correct values.

3.2.2 H_2O molecule

We tested the RT-TDDFT calculation for H_2O molecule by setting different lengths for each time-step. In figure 3.3, time step Δt is set as 0.02 a.u., 0.04 a.u., 0.10 a.u., 0.20 a.u., 0.30 a.u.. All trails have been propagated for 50000 time steps. All other parameters are the same as that of CH_4 molecule calculation. The first 20 excited states obtained from LR-TDDFT calculation are plotted as sticks on each of graphs. Figure 3.3 a,figure 3.3 b,figure 3.3 c, show good agreements of energies of bright states between LR and RT calculation. As numbers of time steps are the same for each trial, the total propagation duration is increasing from 3.3 a to c, so that the peaks in spectrum are sharper and closer to LR results. However, when the size of time step is too large, as in figure 3.3 d and figure 3.3 e, the spectrum is no longer correct. That is caused by the incorrect propagator calculation when time-step is too large.

We also compare the spectrum with different Δt, which is 0.02 a.u. and 0.10 a.u respectively, and with the same total propagation duration $T = 1000\, a.u.$, as shown in figure 3.4. The two spectrums are almost overlapped. Therefore, for water molecule, the current program can give reasonable results up to $\Delta t = 0.10$ a.u..

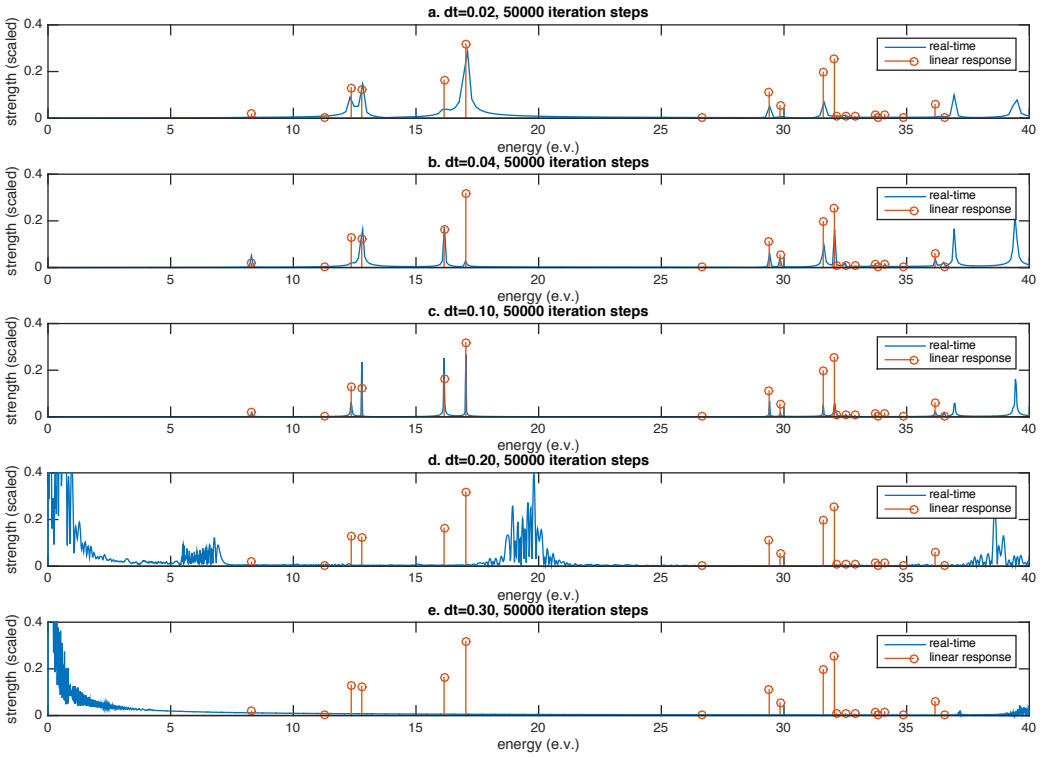

Figure 3.3: Comparison between RT-TDDFT spectrum results and LR-TDDFT results for H_2O with different Δt. Time step Δt is set as 0.02 a.u., 0.04 a.u., 0.10 a.u., 0.20 a.u., 0.30 a.u. respectively. All trails have been propagated for 50000 time steps. All other parameters are the same as that of CH_4 molecule calculation. The first 20 excited states obtained from LR-TDDFT calculation are plotted as sticks. Graph a, b, and c show good agreements of energies for bright states between LR and RT calculation. In graph d and e, the spectrum is no longer correct because of the large time-step.

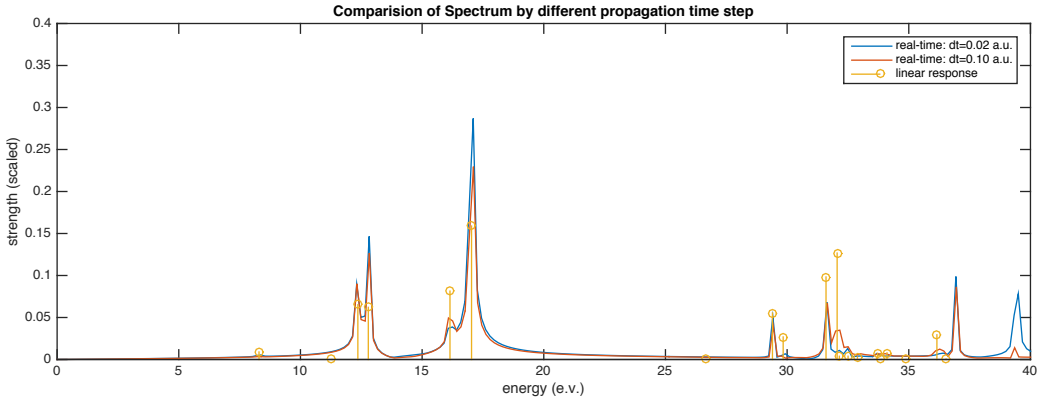

Figure 3.4: Comparison of RT results obtained by Δt =0.02 a.u and Δt =0.1 a.u for H_2O. The current program can give reasonable results up to Δt = 0.10 a.u..

3.2.3 2,3,5-trifluorobenzaldehyde

We tested a larger molecule, 2,3,5-trifluorobenzaldehyde (as in figure 3.5), with basis set 6-31g(d), functional b3lyp, Δt =0.02 a.u., and total propagation duration 12 fs. The LR-TDDFT results are the first 100 excited states shown as sticks. In figure 3.6, the RT results show a good agreement with LR results.

In figure 3.7, we plot the graph with a broaden energy range up to 150 e.V. This shows the capability of RT time calculation that a broad continuous spectrum can be generated. Theoretically, the highest excitation energy to obtain is restricted by $\frac{\pi}{\Delta t}$.

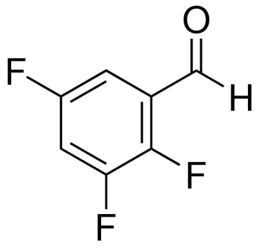

Figure 3.5: 2,3,5-trifluorobenzaldehyde. It is tested with basis set 6-31g(d), functional b3lyp, Δt =0.02 a.u., and total propagation duration 12 fs.

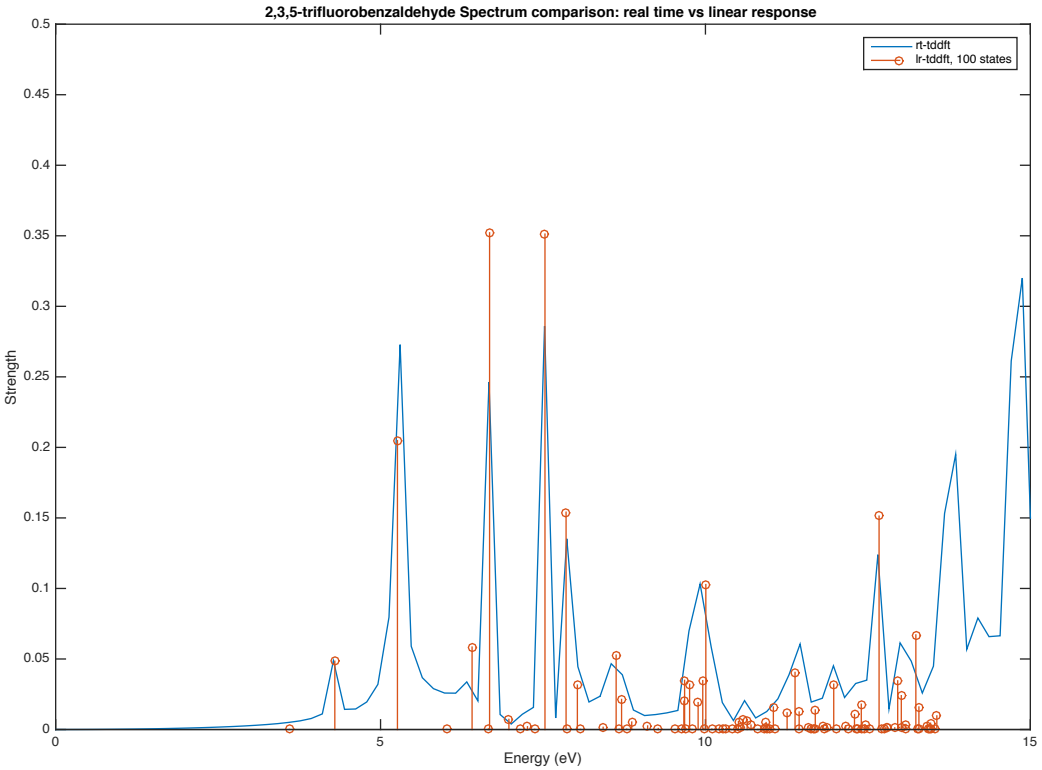

Figure 3.6: Zoomed in graph to compare RT with LR results for 2,3,5-trifluorobenzaldehyde. The LR-TDDFT results are the first 100 excited states, and shown as sticks. The RT results show good agreement with LR results.

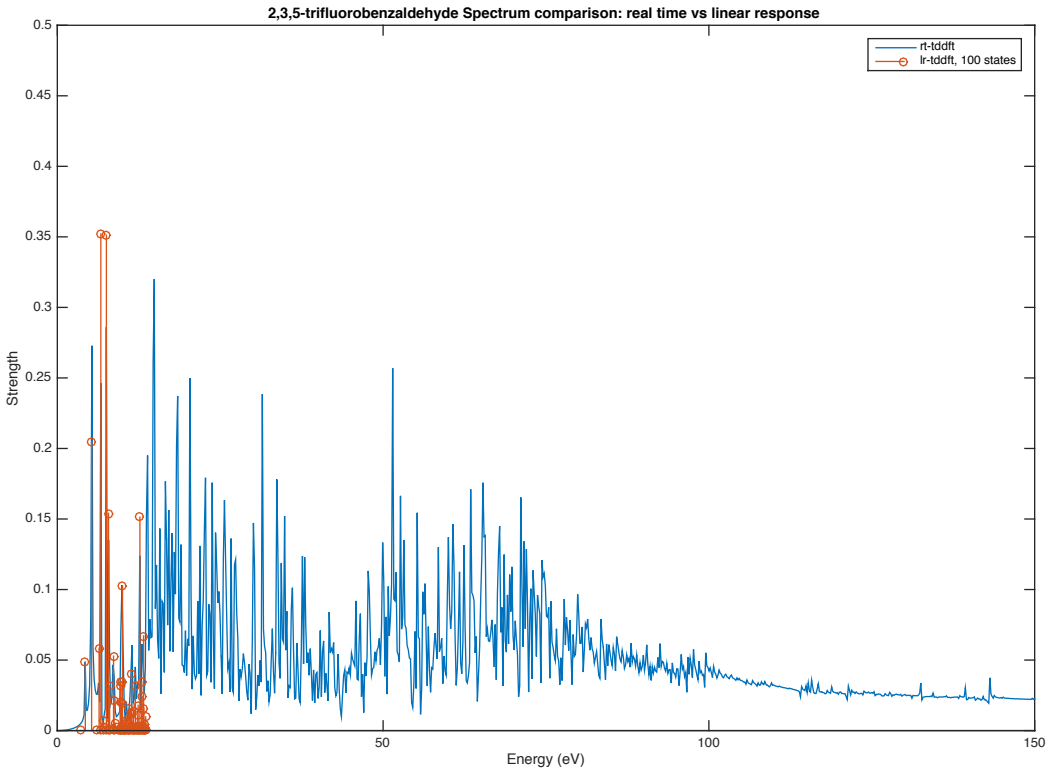

Figure 3.7: The larger scale spectrum for RT and LR results for 2,3,5-trifluorobenzaldehyde. This shows the capability of RT calculation that a broad continuous spectrum can be generated. Theoretically, the highest excitation energy to obtain is restricted by $\frac{\pi}{\Delta t}$.

CHAPTER 4

Conclusions

Results show a good agreement between the real-time calculation and the linear-response calculation in the linear-response regime. The codes for RT-TDDFT in Q-Chem is thoroughly checked. The implemented algorithm is mid-point unitary transformed approximation. We merged the codes of RT-TDDFT into the main develop version of Q-Chem. Since the cost for the real-time calculation is high, propagator algorithms still need to be improved to reach the higher stability and the validity for larger time-step. The parallel of the codes is also needed to be implemented.

Since RT-TDDFT is no longer limited to the weak field, it can be used to study non-linear response of electron systems. The broad, continuous spectrum obtained by RT-TDDFT calculation show the capability to study on high energy excitation, such as x-ray, of molecule systems, which is hard to reach via LR-TDDFT calculation.

What's more, RT-TDDFT is calculated in real-time and real-space, so that the calculation provides direct information on dynamics . For the ultrafast phenomena whose time scale are femtosecond and sub-picosecond, the real-time calculation can

give insight into the dynamics and mechanism. Problems on dynamics in photo-chemistry and electro-chemistry can be studied. For example, the electron injection procedure into the dye-sensitized solar cell can be studied by RT-TDDFT calculation.

Bibliography

[1] Triet S Nguyen and John Parkhill. Nonadiabatic dynamics for electrons at second-order: Real-time tddft and oscf2. *Journal of chemical theory and computation*, 11(7):2918–2924, 2015.

[2] Min Gao, Subhradip Paul, Charles D Schwieters, Zhi-Qiang You, Hui Shao, John M Herbert, Jon R Parquette, and Christopher P Jaroniec. A structural model for a self-assembled nanotube provides insight into its exciton dynamics. *The Journal of Physical Chemistry C*, 119(24):13948–13956, 2015.

[3] Pierre Hohenberg and Walter Kohn. Inhomogeneous electron gas. *Physical review*, 136(3B):B864, 1964.

[4] Walter Kohn and Lu Jeu Sham. Self-consistent equations including exchange and correlation effects. *Physical review*, 140(4A):A1133, 1965.

[5] Erich Runge and Eberhard KU Gross. Density-functional theory for time-dependent systems. *Physical Review Letters*, 52(12):997, 1984.

[6] EKU Gross and Walter Kohn. Local density-functional theory of frequency-dependent linear response. *Physical review letters*, 55(26):2850, 1985.

[7] EKU Gross and W Kohn. Time-dependent density functional theory. *Adv. Quantum Chem*, 21(255):287–323, 1990.

[8] Axel D Becke. Perspective: Fifty years of density-functional theory in chemical physics. *The Journal of chemical physics*, 140(18):18A301, 2014.

[9] Mark E Casida. Response theory for molecules. *Recent Advances in Density Functional Methods:(Part I)*, 1:155, 1995.

[10] Andreas Dreuw and Martin Head-Gordon. Single-reference ab initio methods for the calculation of excited states of large molecules. *Chemical reviews*, 105(11):4009–4037, 2005.

[11] Joachim Theilhaber. Ab initio simulations of sodium using time-dependent density-functional theory. *Physical Review B*, 46(20):12990, 1992.

[12] Kazuhiro Yabana and GF Bertsch. Time-dependent local-density approximation in real time. *Physical Review B*, 54(7):4484, 1996.

[13] Conn ORourke and David R Bowler. Linear scaling density matrix real time tddft: Propagator unitarity and matrix truncation. *The Journal of chemical physics*, 143(10):102801, 2015.

[14] Kenneth Lopata and Niranjan Govind. Modeling fast electron dynamics with real-time time-dependent density functional theory: Application to small molecules and chromophores. *Journal of chemical theory and computation*, 7(5):1344–1355, 2011.

[15] So Hirata and Martin Head-Gordon. Time-dependent density functional theory within the tamm–dancoff approximation. *Chemical Physics Letters*, 314(3):291–299, 1999.

[16] Alberto Castro, Miguel AL Marques, and Angel Rubio. Propagators for the time-dependent kohn–sham equations. *The Journal of chemical physics*, 121(8):3425–3433, 2004.

[17] Xiaosong Li, John C Tully, H Bernhard Schlegel, and Michael J Frisch. Ab initio ehrenfest dynamics. *The Journal of chemical physics*, 123(8):084106, 2005.